Photoluminescent Properties of $ZnO/Zn_{0.8}Mg_{0.2}O$ Nanorod Single-Quantum-Well Structures

Won Il Park, Sung Jin An, Jia Long Yang, and Gyu-Chul Yi*

National CRI center for Semiconductor Nanorods and Department of Materials Science and Engineering, Pohang University of Science and Technology (POSTECH), Pohang 790-784, Korea

Sangsu Hong and Taiha Joo

Department of Chemistry, Division of Molecular and Life Sciences, Pohang University of Science and Technology (POSTECH), Pohang 790-784, Korea

Miyoung Kim

Samsung Advanced Institute of Technology, P.O. Box 111, Suwon 440-600, Korea

Received: August 2, 2004; In Final Form: August 25, 2004

We report on photoluminescent properties of $ZnO/Zn_{0.8}Mg_{0.2}O$ nanorod single-quantum-well structures (SQWs). Catalyst-free metalorganic vapor-phase epitaxy (MOVPE) was employed for precise controls of well widths and compositions of the nanorod SQWs. Both time-integrated and time-resolved photoluminescence (PL) spectra of $ZnO/Zn_{0.8}Mg_{0.2}O$ nanorod SQWs were measured at various temperatures between 10 and 300 K. From the PL spectra of the nanorod SQWs measured at 10 K, a PL peak blue-shift dependent on ZnO well layer width was observed, resulting from a quantum confinement effect. Further photoluminescent properties of the nanorod SQWs were investigated measuring time-resolved PL (TRPL) and temperature-dependent PL spectra.

Recent demonstration of semiconductor nanorod heterostructures opens up significant opportunities for fabrication of electronic and photonic nanodevices on single nanorods.[1−4] In particular, semiconductor nanorod quantum structures with well-defined interfaces are main components for nanoscale resonant tunneling devices, field effect transistors, and light-emitting devices.[1,2] We recently fabricated $ZnO/Zn_{1-x}Mg_xO$ nanorod multiple-quantum-well structures (MQWs) and observed a quantum confinement effect from the nanorod MQWs.[1] Further improvement in fabrication of nanorod heterostructures enables observation of strong room temperature PL even from nanorod SQWs. Although spectral PL of ZnO MQWs has been examined, a complete understanding of the recombination mechanism of carriers requires both temporal and spectral PL measurements. TRPL is a nondestructive and powerful technique for the optical characterization of semiconductors. The exciton lifetime, an important parameter related to material quality and device performance, can be measured by TRPL spectroscopy. Recently, TRPL measurements of ZnO nanorods have shown that the radiative recombination rates of ZnO nanorods, depending on their size, are different from those of ZnO bulk materials.[5] In addition, time-resolved second-harmonic generation and transient PL spectroscopy for ZnO nanowires and nanoribbons have been studied.[6] Nevertheless, TRPL of nanorod heterostructures has not been reported even though TRPL is a powerful technique to investigate exciton dynamics of quantum structures. Here, we report on time-integrated and time-resolved PL properties of $ZnO/Zn_{0.8}Mg_{0.2}O$ nanorod SQWs.

$ZnO/Zn_{1-x}Mg_xO$ nanorod SQWs were fabricated on Al_2O_3-(0001) and Si substrates using catalyst-free MOVPE. Details in the formation of heteroepitaxial structures during nanorod growth have previously been reported.[1] Between each change in composition of the reaction gases during the growth of the nanorod SQWs, the system was purged with pure argon and oxygen, so no layer of mixed composition is expected. Thicknesses and compositions of the $Zn_{1-x}Mg_xO$ layers in the SQWs were determined by transmission electron microscopy (TEM) and energy dispersive X-ray spectroscopy in the TEM chamber. Average concentration of Mg of the $Zn_{1-x}Mg_xO$ layers used in this study was 20 at. %.

Both time-integrated PL (TIPL) and TRPL of the nanorod SQWs were measured at various temperatures between 10 and 300 K for their optical characterizations. The TIPL and TRPL measurements were performed using a continuous wave He−Cd laser (325 nm) and frequency-tripled Ti:sapphire laser (266 nm) as the excitation source, respectively. Details of the PL measurements have been described elsewhere.[6,7]

A schematic of $ZnO/Zn_{0.8}Mg_{0.2}O$ nanorod SQWs is shown in Figure 1a. ZnO well layer thickness (L_w) investigated in this study ranged from 11 to 90 Å while the thicknesses of $Zn_{0.8}Mg_{0.2}O$ bottom and top barrier layers in nanorod SQWs were fixed to 300 and 60 Å, respectively. Electron microscopy images reveal the general morphology of $ZnO/Zn_{0.8}Mg_{0.2}O$ nanorod SQW arrays. As shown in Figure 1, parts b and c, nanorods with a mean diameter of 40 nm were well-aligned vertically over Al_2O_3(0001) substrates. As shown in the inset of Figure 1b, typical mean lengths of $ZnO/Zn_{0.2}Mg_{0.8}O$ nanorod SQWs were investigated to be 970 ± 20 nm. A normalized standard deviation value in length distributions was as small as 0.02, indicating that the nanorod SQWs exhibit the uniform length distribution and also implying uniform ZnO well width distribution.

The detailed structure of the nanorod SQWs was investigated using TEM. Because of composition modulation along the individual nanorod tip ends, *Z*-contrast images of nanorod SQWs

* Corresponding author. E-mail: gcyi@postech.ac.kr.

10.1021/jp046559t CCC: $27.50
Published on Web 09/15/2004

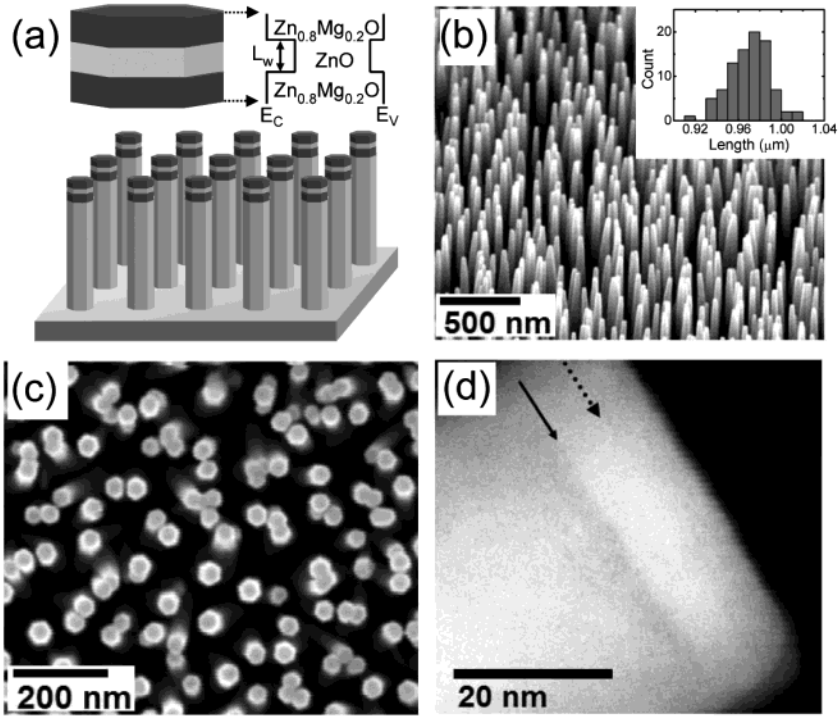

Figure 1. (a) Schematic of nanorod SQW structures consisting of $Zn_{0.8}Mg_{0.2}O/ZnO/Zn_{0.8}Mg_{0.2}O$ on the tips of ZnO nanorods and SQW electronic band diagram. (b) Tilted view and (c) plan view field-emission scanning electron microscopy (FE-SEM) images of nanorod SQWs. (d) TEM image of nanorod SQWs. The inset of part b shows the histograms of nanorod length. Typical mean lengths of $ZnO/Zn_{0.8}Mg_{0.2}O$ nanorod SQWs were estimated to be 970 ± 20 nm.

showed that the contrast change originated from the difference between electron scattering cross sections. As shown in Figure 1d, the *Z*-contrast image exhibits a bright ZnO layer with a thickness of 60 Å between $Zn_{0.8}Mg_{0.2}O$ dark layers. The ZnO layer on $Zn_{0.8}Mg_{0.2}O$ exhibits a very clean and abrupt boundary (indicated by the solid line with an arrow), whereas the interface of $Zn_{0.8}Mg_{0.2}O$ on ZnO (indicated by the dashed line with an arrow) is not so clearly defined, resulting presumably from interface roughness. Further high-resolution TEM (HR-TEM) measurements revealed that the interface roughness increases with ZnO layer thickness, resulting presumably from island growth mode of ZnO on $Zn_{0.8}Mg_{0.2}O$ (data not shown).

Figure 2a shows low-temperature PL spectra of $ZnO/Zn_{0.8}Mg_{0.2}O$ nanorod heterostructure (with $Zn_{0.8}Mg_{0.2}O$ layer thickness of ∼200 nm) and SQWs with different ZnO well layer widths. The nanorod heterostructure exhibited only PL peaks at 3.360 eV (I_2^{ZnO}) and 3.58 eV (I^{ZnMgO}) from ZnO nanorod stems and ZnMgO layers, respectively. No peak was observed between the ZnO and ZnMgO peaks. However, the nanorod SQWs exhibited PL peaks at 3.360−3.366 and 3.375−3.518 eV, and the PL peak energy blue-shifted from 10 to 160 meV as the well layer width decreased from 90 to 11 Å. Furthermore, electroreflectance spectra of the nanorod quantum structures clearly exhibited the existence of the quantized state (data not shown). Variation in the I_{QW} peak energy depending on the ZnO well layer width as well as theoretical predictions in finite square-well potential are depicted in Figure 2b. In this calculation, we employed the following parameters;[8] $0.28m_0$ and $1.8m_0$ for the effective masses of electron and hole in ZnO, respectively, the ratio of conduction and valance band offsets ($\Delta E_c/\Delta E_v$) of 9, and the band gap offset (ΔE_g) of 250 meV. The experimental data agrees well with the results from theoretical calculations, indicating that the systematic increase in the PL emission peak by reducing the well layer width results from the quantum confinement effect.

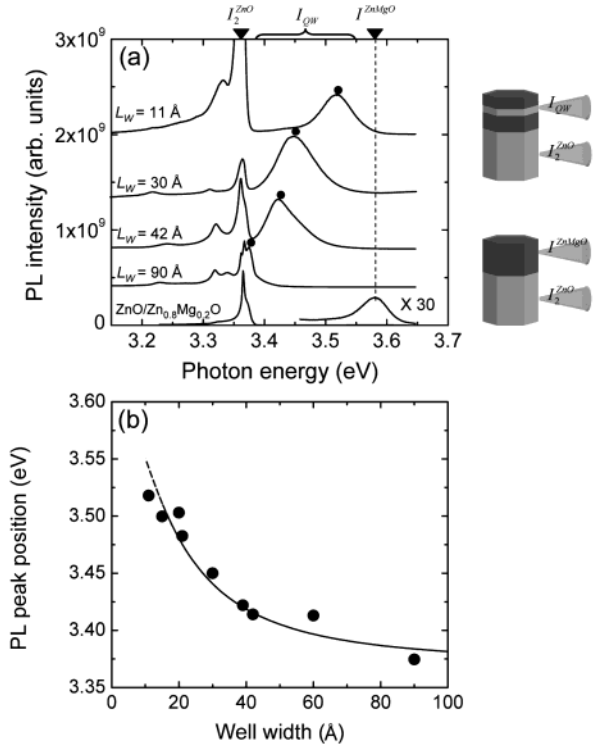

Figure 2. (a) 10 K PL spectra of $ZnO/Zn_{0.8}Mg_{0.2}O$ nanorod heterostructure and SQWs with different ZnO well layer widths and (b) ZnO well layer width vs PL peak energy position in $ZnO/Zn_{0.8}Mg_{0.2}O$ nanorod SQWs (closed circles) and theoretically calculated values (dashed curve).

Further experiments on temperature-dependent evolution of the PL peaks in $ZnO/Zn_{0.8}Mg_{0.2}O$ nanorod SQWs confirms the origin of the PL peaks. Figure 3 exhibits the typical PL spectra of $ZnO/Zn_{0.8}Mg_{0.2}O$ nanorod SQWs with L_w of 30 Å measured

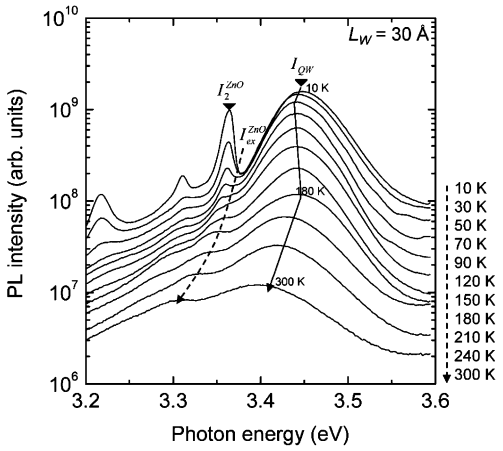

Figure 3. Temperature-dependent PL spectra of $ZnO/Zn_{0.8}Mg_{0.2}O$ SQW nanorods with a well layer width of 30 Å at 10−300 K.

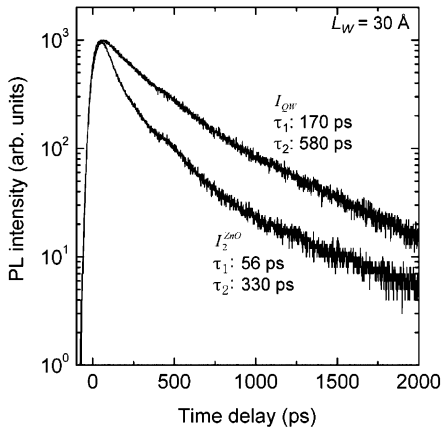

Figure 4. TRPL data of bound exciton (I_2^{ZnO}) emitted from ZnO nanorod stems and I_{QW} emitted from thin ZnO quantum well layers obtained from $ZnO/Zn_{0.8}Mg_{0.2}O$ nanorod SQWs with a well layer width of 30 Å.

in the temperature range from 10 to 300 K. At 10 K, the strong and sharp peak (I_2) due to bound exciton recombination in ZnO nanorod stems was observed at 3.361 eV, while the broad peak (I_{QW}) with a full width at half-maximum of 70 meV appeared at 3.45 eV. The I_{QW} peak originated from the recombination of the excitons at the thin ZnO well layers in the nanorod SQWs. As the temperature increased, the I_2^{ZnO} peak intensity drastically decreased and almost disappeared at temperatures above 90 K, whereas the I_{QW} peak quenched rather slowly and survived even at room temperature.

It is remarkable that the nanorod SQWs showed excellent PL properties including strong room temperature luminescence, even though the nanorod SQWs were grown on Si substrates with a large lattice mismatch with ZnO. Since PL thermal quenching rate is generally dependent on interface quality, the low thermal quenching and strong PL at room temperature implies a high structural quality of SQWs with clean ZnO/ZnMgO interfaces. HR-TEM also confirmed that most defects due to large lattice mismatches were formed at the interface of ZnO/substrate rather than inside nanorod SQWs,[1] which leads to improved interface quality of the ZnO/ZnMgO quantum well layer on nanorods.

The temperature-dependent PL spectra clearly show different temperature-dependent behaviors of I_{ex}^{ZnO}, I_2^{ZnO} and I_{QW} peak positions. The energy positions of free exciton peak (I_{ex}^{ZnO}) and I_2^{ZnO} decreased with band gap energy shrinkage according to the Varshni's formula as generally observed from ZnO bulk crystals and films.[9] However, the I_{QW} emission peak position exhibits so-called "S-shaped" behavior, i.e., a red-blue-redshift of the peak position with increasing temperature.[10] As traced by the solid curve in Figure 3, the I_{QW} peak shows a blueshift of 7 meV in the range of 50−180 K. The blue-shift in the temperature-dependent PL emission is frequently observed from diverse semiconductor thin films with quantum structures and has been explained in terms of localized states or a piezoelectric field (PEF) effect.[10,11]

In addition to the TIPL, TRPL of $ZnO/Zn_{0.8}Mg_{0.2}O$ nanorod SQWs were measured in order to investigate exciton dynamics in nanorod SQWs. Figure 4 shows TRPL signals measured at photon energies of 3.36 and 3.43 eV, which correspond to I_2^{ZnO} emitted from ZnO nanorod stems and I_{QW} emitted from thin ZnO single quantum wells in the nanorods, respectively. Both TRPL data of I_2^{ZnO} and I_{QW} fit well with a double exponential decay curve function with a 25−30 ps rise component. Double-exponential decay behavior was observed from epitaxial ZnO thin films,[12] which strongly suggests that two different decay and/or capture processes are involved in the emission.

The TRPL of I_{QW} shows a slower decay than that of I_2^{ZnO}. From the curve fittings, the decay time constants of I_{QW} are estimated to be 170 and 580 ps, much longer than those of I_2^{ZnO}, 56 and 330 ps. The different PL lifetimes of I_{QW} and I_2^{ZnO} may be explained in terms of size-dependent light−matter interaction in low dimensional nanostructures.[6] In particular, light−matter interaction based on exciton−polariton pictures predicted that radiative recombination time increases as size decreases in cases where particle size is small enough to be comparable to the exciton Bohr diameter.[13] Additionally, the thermal release effect of excitons from localized to delocalized states at the wells might also increase the PL lifetime.[10,14,15]

Even though giant exciton−polariton coupling has been predicted in low dimensional quantum structures,[13] recent experiments have shown strongly quenched excitonic emission of nanoparticles,[14] mainly presumably due to nonradiative processes such as surface state trapping and defect-mediated deep level traps, and multiphonon scattering. In addition, in quantum wells or dots buried in barriers with wider band gaps, carrier leakage through poor heterointerfaces leads to an increase of a nonradiative recombination rate and thus decreases PL lifetimes.[15] From this point of view, it is remarkably noted that the decay time constants (170 and 580 ps) of I_{QW} in nanorod SQWs is comparable to or even longer than those of localized excitons (88−190 ps) measured in a series of ZnO/ZnMgO MQW thin films by Chia et al.[14]

In conclusion, we have measured PL spectra of a series of $ZnO/Zn_{0.8}Mg_{0.2}O$ nanorod SQWs with L_w varying from 11 to 90 Å fabricated on the top surfaces of nanorods using catalyst-free vapor phase epitaxy. From the PL spectra dependent on the ZnO well layer width, a blue-shift of the near-bandedge emission peak was observed, resulting from a quantum confinement effect. Temperature-dependent PL spectra exhibited slow thermal quenching and a red-blue-redshift of the peak position of I_{QW} with increasing temperature. Furthermore, TRPL showed that PL decay time constants of I_{QW} were 170 and 580 ps, larger than those (56 and 330 ps) of I_2^{ZnO}.

Acknowledgment. The authors thank Prof. H. M. Cheong at Sogang University for helpful discussions. This research was performed with the financial support of the National Creative Research Initiative Project and the Center for Nanostructured

Materials Technology under the 21st Century Frontier R&D Program of the Ministry of Science and Technology (MOST), Korea. G.-C.Y. also acknowledges AFSOR (Contract No. FA5209-04-P-0325) for partial financial support. T.J. was supported by the National Research Laboratory program administered by MOST.

References and Notes

(1) Park, W. I.; Yi, G.-C.; Kim, M.; Pennycook, S. J. *Adv. Mater.* **2003**, *15*, 526.

(2) Björk, M. T.; Ohlsson, B. J.; Thelander, C.; Persson, A. I.; Deppert, K.; Wallenberg, L. R.; Samuelson, L. *Appl. Phys. Lett.* **2002**, *81*, 4458.

(3) Gudiksen, M. S.; Lauhon, L. J.; Wang, J.; Smith, D. C.; Lieber, C. M. *Nature* **2002**, *415*, 617.

(4) Wu, Y.; Fan, R.; Yang, P. *Nano Lett.* **2002**, *2*, 83.

(5) Johnson, J.; Knutsen, K. P.; Yan, H.; Law, M.; Yang, P.; Saykally, R. *Nano Lett.* **2004**, *4*, 197.

(6) Hong, S.; Joo, T.; Park, W. I.; Yi, G.-C. *Appl. Phys. Lett.* **2003**, *83*, 4157.

(7) Park, W. I.; Jun, Y. H.; Jung, S. W.; Yi, G.-C. *Appl. Phys. Lett.* **2003**, *82*, 964.

(8) Ohtomo, A.; Kawasaki, M.; Ohkubo, I.; Koinuma, H.; Yasuda, T.; Segawa, Y. *Appl. Phys. Lett.* **1999**, *75*, 980.

(9) Varshni, Y. P. *Physica* **1967**, *34*, 149.

(10) Cho, Y.-H.; Gainer, G. H.; Fischer, A. J.; Song, J. J.; Keller, S.; Mishra, U. K.; DenBaars, S. P. *Appl. Phys. Lett.* **1998**, *73*, 1370.

(11) Bell, A.; Christen, J.; Bertram, F.; Ponce, F. A.; Marui, H.; Tanaka, S. *Appl. Phys. Lett.* **2004**, *84*, 58.

(12) Jung, S. W.; Park, W. I.; Cheong, H. D.; Yi, G.-C.; Jang, H. M.; Hong, S.; Joo, T. *Appl. Phys. Lett.* **2002**, *80*, 1924.

(13) Gil, B.; Kavokin, A. V. *Appl. Phys. Lett.* **2002**, *81*, 748.

(14) (a) Chia, C. H.; Makino, T.; Segawa, Y.; Chia, C. H.; Makino, T.; Segawa, Y.; Kawasaki, M.; Ohtomo, A.; Tamura, K.; Koinuma, H. *J. Appl. Phys.* **2001**, *90*, 3650. (b) Makino, T.; Tuan, N. T.; Sun, H. D.; Chia, C. H.; Segawa, Y.; Kawasaki, M.; Ohtomo, A.; Tamura, K.; Suemoto, T.; Akiyama, H.; Baba, M.; Saito, S.; Tomita, T.; Koinuma, H. *Appl. Phys. Lett.* **2001**, *78*, 1979.

(15) Zeng, K. C.; Li, J.; Lin, J. Y.; Jiang, H. X. *Appl. Phys. Lett.* **2000**, *76*, 3040.

(16) Guo, L.; Yang, S.; Yang, C.; Yu, P.; Wang, J.; Ge, W.; Wong, G. K. L. *Appl. Phys. Lett.* **2000**, *76*, 2901.